BEC BIOENERGETICS COMMUNICATIONS
Bioenerg Commun 2022.19
https://doi.org/10.26124/bec:2022-0019
Open Access

Technical Communication

Cite
Vera-Vives AM, Perin G, Morosinotto T (2022) High-resolution photosynthesis-irradiance curves in microalgae. Bioenerg Commun 2022.19. https://doi.org/10.26124/bec:2022-0019

Author contributions
Data collection was performed by AMVV. Data analysis was done by AMVV and GP. TM and GP conceived and designed the experiments. All authors wrote the manuscript.

Conflicts of interest
Tomas Morosinotto was registered as a key opinion leader by Oroboros Instruments for testing new developments of the NextGent-O2k.

Received 2022-05-05
Reviewed 2022-07-18
Revised 2022-10-12
Accepted 2022-12-13
Published 2022-12-15

Open peer review
Sabine Schmitt (editor)
Thomas Roach (reviewer)
Lijin Tian (reviewer)

High-resolution photosynthesis-irradiance curves in microalgae

Antoni M Vera-Vives, Giorgio Perin, Tomas Morosinotto*

Department of Biology, University of Padova, Italy

* Corresponding author: tomas.morosinotto@unipd.it

Summary

The rate of oxygen evolution provides valuable information on the metabolic status and photosynthetic performance of a cell, and it can be quantified by means of a photosynthesis-irradiance (PI) curve. Up to now, the construction of PI curves of unicellular organisms based on oxygen evolution has been difficult and time consuming due to the lack of sensitive instruments. Here we describe the setup of a reproducible method for constructing PI curves based on oxygen evolution using small amounts of sample in the microalga *Nannochloropsis gaditana*, easily translatable to other algal species.

Keywords – photosynthesis, microalgae, oxygen evolution

1. Introduction

Photosynthetic eukaryotic organisms rely on two organelles, chloroplasts and mitochondria, for the synthesis of the molecules fuelling their metabolism, NAD(P)H and ATP. The two organelles share common features such as membrane-bound enzymatic complexes implicated in electron transfer coupled to proton translocation and the generation of a protonmotive force driving the synthesis of ATP.

In chloroplasts, light energy fuels the electron transfer from water to $NADP^+$ to generate NADPH via photosystem II (PSII), cytochrome b_6f (Cyt b_6f) Complex and photosystem I (PSI), generating oxygen as by-product. The electron transfer is coupled to proton translocation from the chloroplast stroma into the thylakoid lumen and

establishes a transmembrane electrochemical potential, exploited by the ATP synthase for the synthesis of ATP in a process called photophosphorylation.

Photosynthetic eukaryotes contain mitochondria, where electrons are transferred from the substrates NADH and succinate to molecular oxygen O_2. In the dark, respiration is responsible for cells energy supply, but respiration also occurs in the light, when its activity is important for carbon fixation and optimal photosynthesis (Bailleul et al 2015).

In the same way that O_2 consumption is used as a proxy for quantifying respiratory activity and electron transfer through the mitochondrial electron transfer system (ETS), photosynthetic activity and the rate of electron transfer through the plastidial electron transfer system (pETS) can be quantified by the rate of O_2 evolution.

Oxygen evolution and, hence, the photosynthetic rate, depend on light intensity. At low intensities, photosynthesis is limited by the light availability and thus the energy to drive electron transfer. Therefore, in this range, the relationship between light intensity and electron transfer (and thus O_2 evolution) is linear. This linearity is lost at elevated light intensities where other factors (i.e. rate of carbon fixation) become limiting for photosynthesis and any further increase of photons does not result in a higher rate of electron transfer. On the contrary, when photosynthesis is saturated at high intensities, light excess can drive the generation of reactive oxygen species (ROS) and photoinhibition.

This relationship between light intensity and photosynthetic rate is depicted by the so-called photosynthesis-irradiance (PI) curve. Historically, the proxy for photosynthesis quantification in microalgae has been the rate of carbon fixation measured as ^{14}C-carbon assimilation (for examples see Jassby, Platt 1976; Perry et al 1981). Another proxy for PI curves is the rate of O_2 evolution, as O_2 is directly proportional to the number of electrons that move through the pETS. Compared to CO_2, which is only indirectly linked to the transfer of electrons as other metabolic pathways compete for the ATP and reducing power, O_2 is a better proxy for building PI curves. Quantification of O_2 was done first with the so-called clear and dark bottle method (Strickland, 1960), and then using low-resolution devices based on Clark-type sensors. However, these techniques have limitations due to the difficulty in precisely controlling the amount of light that reaches the sample. In addition, they usually require elevated concentrations of cells, which can cause inhomogeneity due to internal shading.

The high resolution of the NextGen-O2k with the PhotoBiology module (PB-Module) enable construction of PI curves with an unprecedented accuracy (Huete-Ortega et al 2020; Went et al 2021). The increased resolution comes from the two components of the system. First, the core O2k-FluoRespirometer is more sensitive than any of the other Clark sensor-based oxygraphs (Gnaiger 2008) commonly used in plant and algal research. This makes it possible to perform measurements of oxygraphy using a very small amount of sample, as we demonstrate in this work. Second, the PB-Module permits fine-tuning of the light intensity that reaches the sample. The combination of these two factors allow PI curves to be obtained in a fast and reproducible manner.

In this work we (*1*) analyze the ability of the NextGen-O2k to build PI curves with high resolution quickly and using low amounts of material and (*2*) titrate different cell concentrations to check for consistency and reproducibility of the measurements.

We use as a model the oleaginous alga *Nannochloropsis gaditana*, an heterokont that is gaining interest for its industrial applications.

2. Methods

2.1. Algal cultures

Nannochloropsis gaditana, strain CCAP 849/5, was purchased from the Culture Collection of Algae and Protozoa (CCAP) and maintained in F/2 solid media, with 32 $g \cdot L^{-1}$ sea salts (Sigma Aldrich), 40 mM Tris-HCl (pH 8), Guillard's (F/2) marine water enrichment solution (Sigma Aldrich), 1 % agar (Duchefa Biochemie). Cells were pre-cultured in sterile F/2 liquid media in Erlenmeyer flasks irradiated with 100 µmol photons$\cdot s^{-1} \cdot m^{-2}$, 100 rpm agitation, at 22 ± 1 °C in a growth chamber. Growth curves started from a cell-count concentration of $5 \cdot 10^6$ x$\cdot mL^{-1}$ in F/2 supplemented with 10 mM $NaHCO_3$ to avoid carbon limitation and were kept in the same growth conditions of pre-cultures.

2.2. Cell counting

Cell concentration was monitored on the fourth day of the growth curve with an automatic cell counter (Cellometer Auto X4, Cell Counter, Nexcelom) to collect the different numbers of cells needed for high-resolution respirometry. For high concentrations, cells were collected via mild centrifugation at 3500 *g* for 10 minutes at room temperature.

2.3. High-resolution respirometry

Oxygen consumption and production were measured on the fourth day of the growth curve. Measurements were performed at 22 °C using a test version of the NextGen-O2k and the PB-Module (Oroboros Instruments, Innsbruck) with the software DatLab 7.4.0.4 (Went et al 2021). The O2k-chambers were magnetically stirred at 750 rpm and the O_2 concentration of the chambers was measured at a data sampling interval of 2 seconds. The PB light source contained a blue OSLON® LED (emitting wavelength range 439-457 nm with the peak at 451 nm, manufactured by OSRAM) attached to the window of the NextGen-O2k chamber.

The 2 mL chambers were filled with growth medium containing 5 mM $NaHCO_3$ to avoid carbon limitation during the measurement and equilibrated to experimental temperature (22 °C) for a few minutes. Then, a small fraction of medium was replaced with an aliquot of cell suspension to reach the desired final concentration in the chamber. The chambers were then closed and the O_2 consumption rate at dark was monitored.

2.4. Light curve protocol

After stabilization of dark respiration, the light source was turned on at 10 µmol photons$\cdot s^{-1} \cdot m^{-2}$ until stabilization of the O_2 flow, typically 5-10 min (Figure 1). This was done recursively for the following light intensities: 10, 25, 50, 75, 100, 150 and 200 µmol photons$\cdot s^{-1} \cdot m^{-2}$. The reported values of O_2 evolution rates at each intensity correspond to the median of 40-50 points in the stable region of oxygen flow (pink regions in Figure 1A). The protocol was automated by running a DatLab 7 script, with an initial period of 600 s for measurement of dark respiration, followed by 300 s intervals at the light intensities shown above, and a final phase of dark respiration in both chambers.

2.5. Data analysis

After each experiment, the raw data were exported from DatLab and analyzed with a spreadsheet template provided by Oroboros Instruments. For building PI curves, we used the O_2 flow normalized to cell concentration expressed in million cells: pmol $O_2 \cdot s^{-1} \cdot 10^{-6}$ x = amol $\cdot s^{-1} \cdot x^{-1}$.

The data were fitted with the equation defined in Ye (2007) using a minimum mean square error-based approach with OriginPro Version 2020b (OriginLab Corporation, Northampton, MA, USA)

$$P_N = \Phi_{(I_0-I_{comp})} \times \frac{1-\beta \cdot I}{1+\gamma \cdot I} \cdot (I-I_{comp})$$

where: P_N is the net O_2 photosynthetic rate per 10^6 cells [pmol $\cdot s^{-1} \cdot 10^{-6}$ x]; $\Phi_{(I_0-I_{comp})}$ is the quantum yield in the range between I_0 and I_{comp} [pmol $O_2 \cdot m^2 \cdot$µmol photons$^{-1} \cdot 10^{-6}$ x]; β and γ are two adjusting factors (dimensionless); I is the photosynthetic photon flux density [µmol photons $\cdot s^{-1} \cdot m^{-2}$] and I_{comp} is the light compensation point [µmol photons $\cdot s^{-1} \cdot m^{-2}$]. Further three derived parameters were calculated: R_D, the dark O_2 respiration rate [pmol $\cdot s^{-1} \cdot 10^{-6}$ x]; P_{gmax}, the maximal gross O_2 photosynthetic rate [pmol $\cdot s^{-1} \cdot 10^{-6}$ x], and I_{sat}, the light saturation point [µmol photons $\cdot s^{-1} \cdot m^{-2}$]. These three parameters were derived as follows:

$$R_D = \Phi_{(I_0-I_{comp})} \cdot I_{comp} \qquad P_{gmax} = P_N + R_D \qquad I_{sat} = \frac{\sqrt{\frac{(\beta+\gamma)\cdot(1+\gamma \cdot I_{comp})}{\beta-1}}}{\gamma}$$

3. Results

3.1. Establishment of a protocol for PI curves

First tests were run with different cell concentrations, observing that $5 \cdot 10^6$ x $\cdot mL^{-1}$ to $10 \cdot 10^6$ x $\cdot mL^{-1}$ were sufficient to obtain traces of good quality as shown in Figure 1.

At a working cell-count concentration of $10 \cdot 10^6$ x $\cdot mL^{-1}$ (corresponding to 0.8 µg Chl $\cdot mL^{-1}$, see the corresponding plot in Figure 2), the rate of dark respiration was estimated as 0.95 ± 0.16 pmol $O_2 \cdot s^{-1} \cdot mL^{-1}$. We increased light intensity progressively starting from 10 µmol photons $\cdot s^{-1} \cdot m^{-2}$. After each light increase the O_2 flux stabilized within 2-4 minutes. The light compensation point, I_{com}, (*i.e.* the point at which net photosynthesis is null) was estimated to be 9.5 ± 1.2 µmol photons $\cdot s^{-1} \cdot m^{-2}$, while saturation was reached at 149 ± 37 µmol photons $\cdot s^{-1} \cdot m^{-2}$.

From first experiments as the one reported in Figure 1, we established and automated a protocol to increase the light every 5 minutes, followed for all measurements reported hereinafter:

1) Add the sample into the chamber.
2) Wait for 10 minutes to measure dark respiration.
3) Turn light on at 10 µmol photons $\cdot s^{-1} \cdot m^{-2}$.
4) Measure for 5 minutes.

5) Increase the light to 25 µmol photons·s^{-1}·m^{-2} followed by 50, 75, 100, 150, 200 µmol photons·s^{-1}·m^{-2}, measuring for 5 minutes after each light change. These intervals were chosen as the most informative to describe the PI curve shape.
6) Wash the chambers and start next experiment.

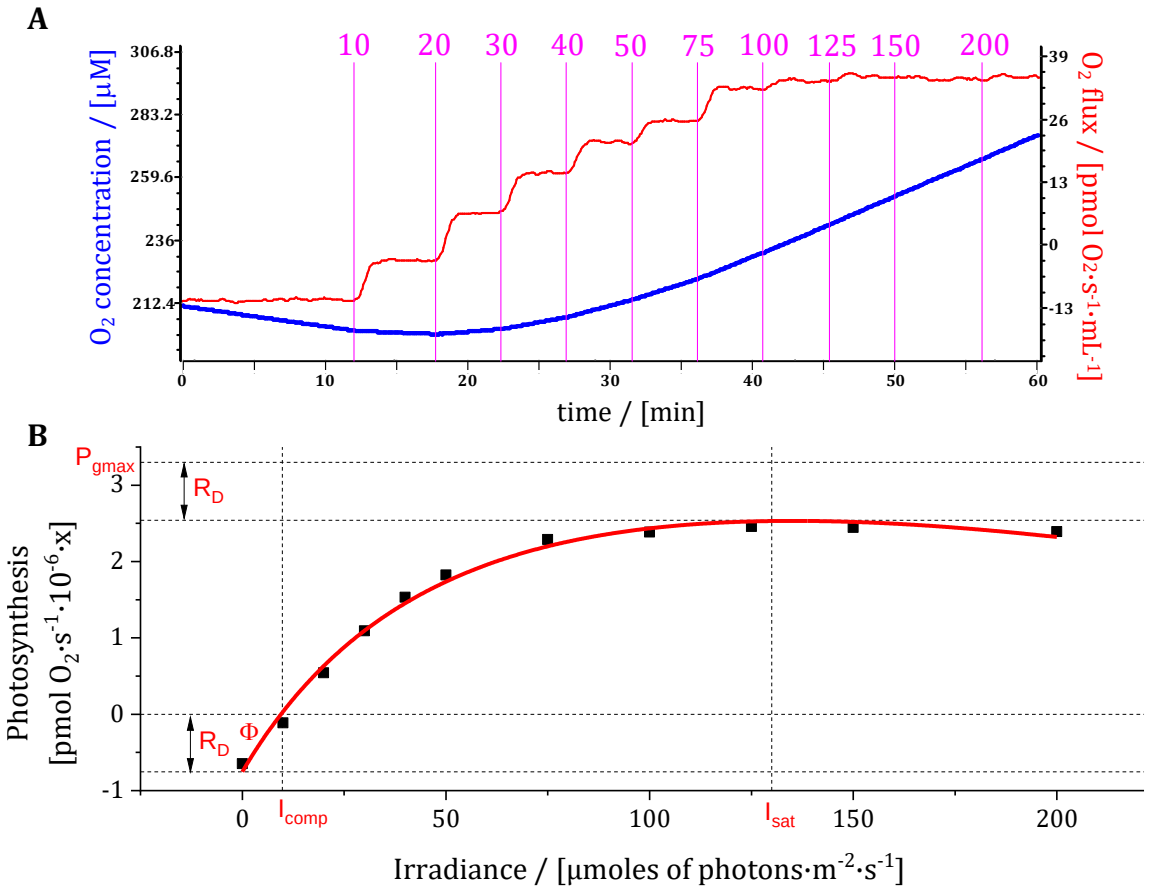

Figure 1. Construction of a PI curve. (A) Simplified diagram of a typical experiment as visualized by DatLab. After each increase in light intensity (vertical lines, values in µmol photons·s^{-1}·m^{-2}), the O_2 flux (red plot, background-corrected time-derivative of O_2 concentration in blue) first increases and then stabilizes. At high light intensities a plateau is reached. **(B)** Fitting of a PI curve to the data reported in A. Each point represents the median of 30-40 datapoints of the stable region of O_2 flux at each intensity (pink segments in A).

A complete experiment lasted less than 1 h, allowing us to perform up to 10 experiments per day, each in two replicas, in the two chambers. It is worth noting that the parameters derived from the PI curves are not influenced by the initial O_2 concentration, given every experiment starts after equilibration of the incubation medium with atmospheric oxygen (Figure 1).

3.2. Testing the effect of cell concentration on PI curves

Once we defined our experimental protocol, we performed different sets of measurements to check for the ideal range of cell concentrations. In our samples, the chlorophyll content was approx. 0.08 µg of chlorophyll per million cells. It should be

mentioned that *Nannochloropsis* cells are quite small (diameter of 2-3 µm). Working concentrations with other microalgae such as *Chlamydomonas*, that have a 10 µm diameter and thus approx. 50 times larger cell volume, should be approx. 25-50 times smaller in terms of cell count.

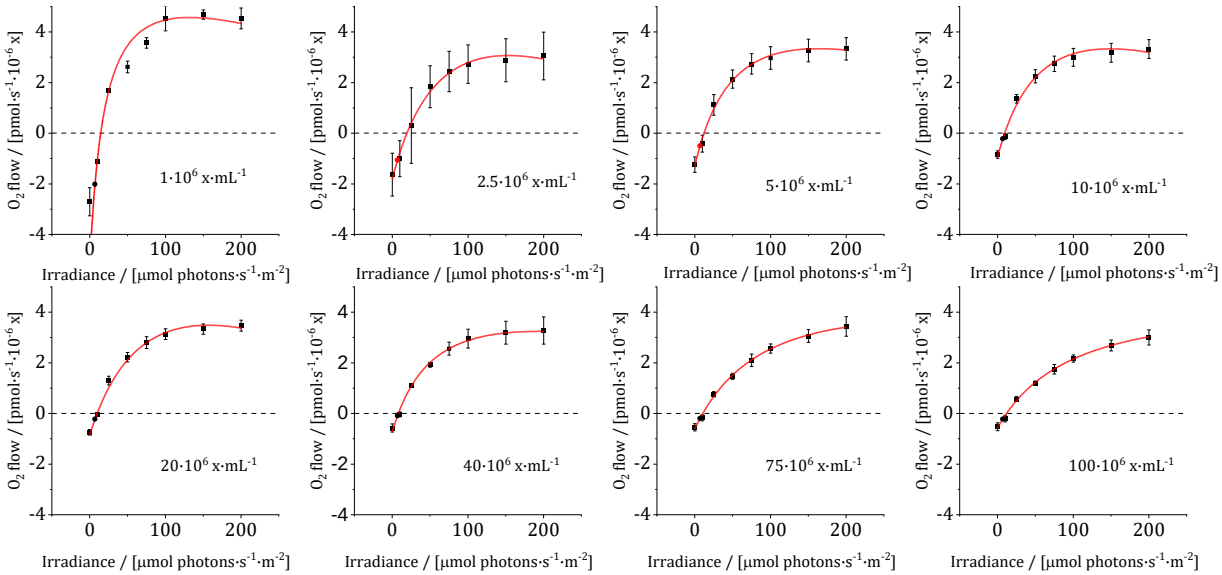

Figure 2. PI curves at cell concentrations ranging from 2.5·10⁶ x·mL⁻¹ to 100·10⁶ x·mL⁻¹. Each data point is the mean of 4 replicates, and the error bars correspond to the standard error.

We tested the following cell concentrations (10^6 x·mL^{-1}): 1, 2.5, 5, 10, 20, 40, 75 and 100. The respective PI curves are shown in Figure 2. Lower concentrations were also tested but were not retained as the low volume-specific flux was too noisy. In all considered cases, the data points followed the expected shape represented in Figure 1B and could be fitted accurately with our PI model. The values of photosynthetic parameters are reported in Table 1.

Table 1. Photosynthetic parameters at different cell concentrations. Values correspond to the mean of four replicates ± standard error. Please refer to the methods section for the description of the meaning of all parameters.

Cell concentration (10^6 x·mL^{-1})	$\Phi_{(I_0\text{-}I_{comp})}$	I_{com}	I_{sat}	R_D	P_{gmax}
1	0.36 ± 0.10	14.6 ± 0.5	133 ± 59	5.28 ± 1.29	9.9 ± 1.2
2.5	0.09 ± 0.02	19.5 ± 2.3	153 ± 21	1.82 ± 0.21	4.9 ± 0.2
5	0.11 ± 0.01	12.2 ± 1.1	163 ± 27	1.31 ± 0.12	4.6 ± 0.2
10	0.1 ± 0.02	9.5 ± 1.2	149 ± 37	0.95 ± 0.16	4.3 ± 0.3
20	0.09 ± 0.01	9.9 ± 0.7	157 ± 26	0.85 ± 0.12	4.3 ± 0.2
40	0.08 ± 0.01	8.3 ± 1.2	175 ± 29	0.64 ± 0.13	3.9 ± 0.2
75	0.05 ± 0.01	10.8 ± 1.4	329 ± 288	0.59 ± 0.1	4.2 ± 0.7
100	0.05 ± 0.01	12.2 ± 1.2	347 ± 263	0.56 ± 0.08	3.8 ± 0.6

Three groups of concentrations could be defined. First, for $1{\cdot}10^6$ x·mL^{-1} and $2.5{\cdot}10^6$ x·mL^{-1}, data variability was larger, especially at low light intensities where O_2 flux per volume [pmol·s^{-1}·mL^{-1}] was low, affecting the signal-to-noise ratio. These cell

concentrations are not optimal, even though these limitations could be addressed by increasing the number of experimental replicates and prolonging sampling times.

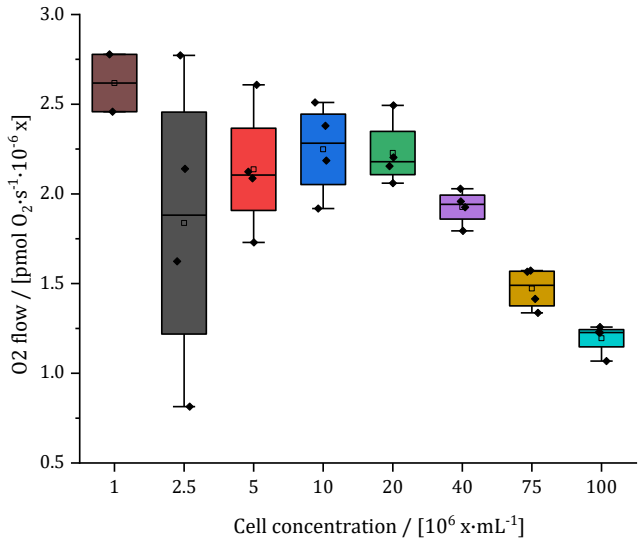

Figure 3. Comparison of O_2 flow at a mid-light intensity (50 µmol photons·s^{-1}·m^{-2}) at different cell concentrations.

Second, the cell concentration range comprised between $5{\cdot}10^6$ x·mL^{-1} and $20{\cdot}10^6$ x·mL^{-1} showed no major differences in terms of curve shape or internal variability among replicas. Since O_2 evolution was normalized to the number of cells, this consistency suggest that the measurements are stable and not influenced by the cell concentration in this range (Figure 3). This also suggests that light shading is not affecting the measurements. Concentrations within this range seem optimal for future PI curve experiments.

Last, for $40{\cdot}10^6$ x·mL^{-1} to $100{\cdot}10^6$ x·mL^{-1}, there was instead an effect due to the cell concentration, especially during the linear phase (Figure 3). The light saturation point was higher with higher concentrations, likely explained by a shading effect between cells at higher concentrations due their high optical density that caused an inhomogeneous light distribution in the sample. This hypothesis was confirmed by the observation that P_{gmax} was the same for all concentrations (Table 1). This suggests that even at high cell concentrations the value of maximal photosynthesis is correctly estimated because self-shading is not a factor anymore when light is in excess.

4. Conclusions

Our results demonstrate that the protocol developed for building PI curves of *Nannochloropsis gaditana* cultures with the NextGen-O2k is robust and reproducible. The possibility of making programmed light changes enables multiple measurements with limited time and efforts. The ideal working cell concentrations are those in the range of $5{\cdot}10^6$ x·mL^{-1} to $10{\cdot}10^6$ x·mL^{-1}, corresponding to 0.4-0.8 µg Chl·mL^{-1}. This concentration is more than 30 times lower than the one we used in the past with a classical Clark sensor (Perin et al 2015). In our conditions, a 20 mL 4 day-old culture of *Nannochloropsis* had typically a cell concentration of $25{\cdot}10^6$ x·mL^{-1} to $45{\cdot}10^6$ x·mL^{-1}. Therefore, a single measurement needed a volume of culture of 200-800 µL, less than 0.1 % of the total culture volume. Consequently, the same culture can be used for other experiments, optimizing its use. This is of particular interest for strains with a reduced growth rate. The reproducibility of our approach makes it possible to compare the photosynthetic performance of different strains and mutants under various experimental conditions.

Another major advantage of working with low concentrations is that it is possible to work in a range where self-shading effects are negligible. This is particularly important to study the effect of light intensity on the photosynthesis parameters.

Acknowledgements

This work was supported by project NextGen-O2k which has received funding from the European Union's Horizon 2020 research and innovation programme under grant agreement Nº 859770 (Oroboros Instruments).

References

Bailleul B et al (2015) Energetic coupling between plastids and mitochondria drives CO_2 assimilation in diatom. https://doi.org/10.1038/nature14599

Gnaiger E (2008) Polarographic oxygen sensors, the oxygraph and high-resolution respirometry to assess mitochondrial function. https://doi.org/10.1002/9780470372531.ch12

Huete-Ortega M, Di Marcello M, Iglesias-Gonzalez J, Gnaiger E (2020) High-resolution respirometry for chloroplast and mitochondrial bioenergetics in Chlamydomonas reinhardtii — towards biotechnology exploitations. https://doi.org/10.26124/mitofit:ea20.algaeurope.0001

Jassby AD, Platt T (1976) Mathematical formulation of the relationship between photosynthesis and light for phytoplankton. https://doi.org/10.4319/LO.1976.21.4.0540

Perin G, Bellan A, Segalla A, Meneghesso A, Alboresi A, Morosinotto T (2015) Generation of random mutants to improve light-use efficiency of Nannochloropsis gaditana cultures for biofuel production. https://doi.org/10.1186/s13068-015-0337-5

Perry MJ, Talbot MC, Alberte RS (1981) Photoadaption in marine phytoplankton: Response of the photosynthetic unit. https://doi.org/10.1007/BF00388170

Strickland J (1960) Measuring the production of marine phytoplankton. https://waves-vagues.dfo-mpo.gc.ca/library-bibliotheque/10157.pdf

Went N, Di Marcello M, Gnaiger E (2021) Oxygen dependence of photosynthesis and light-enhanced dark respiration studied by High-Resolution PhotoRespirometry. https://doi.org/10.26124/mitofit:2021-0005

Ye ZP (2007) A new model for relationship between irradiance and the rate of photosynthesis in *Oryza sativa*. https://doi.org/10.1007/s11099-007-0110-5